

Cite this: *RSC Adv.*, 2014, 4, 26912

Redox properties of LDH microcrystals coated with a catechol-bearing phosphonate derived from dopamine†

Maria de Victoria Rodríguez,^a Ernesto Brunet,^a Morena Nocchetti,^b
Federica Presciutti^c and Ferdinando Costantino^{*cd}Received 22nd April 2014
Accepted 10th June 2014

DOI: 10.1039/c4ra03660c

www.rsc.org/advances

The surface of Zn–Al-chloride LDH microcrystals (LDH = Layered Double Hydroxides) was activated by grafting a redox active catechol bearing bis-phosphonate obtained by dopamine derivatization. The obtained phosphonate uniformly coats the LDH crystals surface and the catechol groups are exposed. The redox activity of the catechol was employed for the quick and easy synthesis of Gold NPs, which are supported onto the LDH microcrystal surface. The synthetic procedures and the complete characterization of the hybrid system are reported.

Introduction

Catechol bearing molecules can be found in a very high number of natural and biological processes, including neurosignalling,¹ photoprotection,² metal complexation,³ and surface adhesion.⁴

The latter characteristic is typical of dopamine (3,4-dihydroxyphenylalanine) which is responsible of the mussel foot protein adhesion. This feature has been recently employed as bio-mimetic tool for the design of highly adhesive mussel inspired films and materials, thanks to the facile polymerization of dopamine into polydopamine. The catechol-redox activity of the dopamine was also recently used to induce the reduction of noble metals into metal nanoparticles (NPs) giving rise to several hybrid systems, based on polydopamine polymer and noble metal NPs.⁵ Among them we can cite the synthesis of adhesive mussel-inspired films containing Au and Ag NPs with high conductive properties,⁶ with antimicrobial activity⁷ and core-shell system for imaging and antitumoral activity.⁸

Actually, one of the major challenges of this chemistry is focused on the coupling of such active hybrid systems with other materials which can act both as solid support and that could embody an added value due to their intrinsic properties (such as TiO₂, graphene, carbon nanotubes and so on). Among

2D materials, layered double hydroxides (LDHs) epitomize one of the most prevalent compounds actually used for a huge number of applications such as catalyst in many processes,⁹ controlled drug delivery systems,¹⁰ gas capture,¹¹ water purifier¹² or in biomedical applications.¹³

Herein we report on the surface modification of well crystallized ZnAl-LDH microcrystals achieved by grafting it with a catechol-bearing phosphonate derived from dopamine, in order to impart redox properties to the system. The redox properties of this new hybrid system were then employed for the synthesis of gold nanoparticles (AuNPs) stabilized onto the LDH surface through the oxidation to quinone of the catechol groups exposed on the surface.

Experimental

Instrumental details

XRPD patterns for Rietveld refinements were collected with Cu K α radiation on a PANalytical X'PERT PRO diffractometer, PW3050 goniometer equipped with an X'Celerator detector. The long fine focus (LFF) ceramic tube operated at 40 kV and 40 mA. To minimize preferential orientations of the microcrystals, the samples were carefully side-loaded onto an aluminum sample holder with an oriented quartz monocrystal underneath. Thermogravimetric (TG) measurements were performed using a Netzsch STA490C thermoanalyser under a 20 mL min⁻¹ air flux with a heating rate of 5 °C min⁻¹. FE-SEM images were collected with a LEO 1525 ZEISS instrument working with an acceleration voltage of 15 kV. TEM images were collected with Philips 208 Transmission Electron Microscope (TEM). A small drop of the dispersion was deposited on a copper grid that had been pre-coated with a Formvar film and then evaporated in air at room temperature (r.t.). UV-vis spectrometry was performed by using a Deuterium-Halogen lamp as excitation source, (emitted light

^aDepartamento de Química Orgánica, Facultad de Ciencias, Universidad Autónoma de Madrid, 28049 Madrid, Spain

^bDipartimento di Scienze Farmaceutiche, University of Perugia, Via del Liceo 1, 06123, Perugia, Italy

^cDipartimento di Chimica, Biologia e Biotecnologie, University of Perugia, Via Elce di Sotto 8, 06123, Perugia, Italy

^dCNR – ICCOM, Via Madonna del Piano 10, Sesto Fiorentino, 50019, Firenze, Italy. E-mail: ferdinando.costantino@unipg.it

† Electronic supplementary information (ESI) available: Complete synthetic procedures, Rietveld refinement details, FT-IR spectra. See DOI: 10.1039/c4ra03660c

from 200 to 1100 nm) and a high sensitive CCD spectrometer (Avaspec 2048 USB2, 200–1100 nm range, spectral resolution 8 nm). Three single 400 micron core fibres directed the light from the source to the analysing surface. ^1H and ^{13}C spectra were recorded on Bruker AV-300 (300 MHz, 75.5 MHz respectively), ^{31}P and ^{19}F -NMR spectra were recorded on Bruker AVII-300 (121 MHz and 282 MHz respectively) in the indicated solvents. Transmittance mid-FT-IR measurements were carried out with a JASCO FT/IR 4000 spectrophotometer. The spectral range collected was 400 to 4000 cm^{-1} , with a spectral resolution of 2 cm^{-1} acquiring 100 scans. The samples were dispersed on anhydrous KBr pellets. Metal and phosphorus analyses were performed with Varian 700-ES series inductively coupled plasma-optical emission spectrometers (ICP-OES). A weighted amount of the samples (about 10 mg) was dissolved in concentrate HCl/HNO_3 3/1 v/v and the solution was brought to a final volume of 50 mL. The solution properly diluted was analyzed by ICP. Elemental analysis were also performed on a LECO CHNS-932 analyzer in the Sidi, UAM. Total Reflection X-Ray Fluorescence (TXRF) measurements were performed on a 8030C Atomika spectrometer using a direct solid method. The spectrometer is equipped with a X-ray tube of 3 kW and a multilayer monochromator. The measurements were performed using 50 kV, 8500 cps of speed and time acquisition of 500 s. The microwave equipment was a Biotage initiator 2.5.

Syntheses

Synthesis of $\text{H}_4\text{P}_2\text{O}_6\text{DOPA}$

$\{[2-(3,4\text{-Dihydroxyphenyl)ethyl}]\text{imino}\}\text{di}(\text{methylene})\text{bis}(\text{phosphonic acid})$, hereafter $\text{H}_4\text{P}_2\text{O}_6\text{DOPA}$, was prepared by a modified Mannich type reaction¹⁴ starting from a doubly protected dopamine. The procedure involved the protection of both catechol and the amino groups in order to prevent polymerization of the dopamine and the formation of π -conjugated complexes like quinidrone.

One of the main problems of catechol is its quick oxidation to the quinone form. Due to this, the key step in the synthesis of the $\text{H}_4\text{P}_2\text{O}_6\text{DOPA}$ is the protection of this group in order to avoid oxidation. In the presence of an amino group direct protection of a catechol group, by acetonide formation is not possible due to the high reactivity of the amino group thus forcing its protection first. The procedure of this initial stage was performed at room temperature by treating dopamine hydrochloride with methyl trifluoroacetate in methanol in the presence of triethylamine.¹⁵ This protection would be easily removed as shown later on in the scheme. Then, the catechol group was protected building the aforementioned acetonide in high yield by refluxing trifluoroacetate-dopamine with 2,2-dimethoxypropane (DMP) in the presence of a catalytic amount of *p*-toluenesulfonic acid (*p*-TsOH). In order to shift the equilibrium reaction, the water formed was removed with a soxhlet extractor filled with CaCl_2 or activated molecular sieves. Once the catechol is protected, the next step is the introduction of the anchoring phosphonic groups so that the amino protection needs to be removed, maintaining catechol's. Once more, this reaction was performed at room temperature under very mild conditions using LiOH in a $\text{H}_2\text{O}/\text{THF}$ solution. Then the diphosphonate

anchoring group can be introduced. However, conventional Irani synthesis cannot be directly carried out by using formaldehyde and H_3PO_3 because, in those strong acidic conditions, deprotection of catechol and its polymerization readily occurs. Therefore, a modified Irani reaction has been performed by refluxing acetonide-protected dopamine in the presence of paraformaldehyde and diethylphosphite.¹⁶ The last stage in the synthesis of $\text{H}_4\text{P}_2\text{O}_6\text{DOPA}$ is the hydrolysis of phosphonate groups and deprotection of catechol that was performed on a single step by refluxing in concentrated HCl . Scheme 1 briefly summarizes the synthetic routes with the yields, whereas the full detailed procedure is reported in the ESI.†

Synthesis of ZnAl-chloride LDH

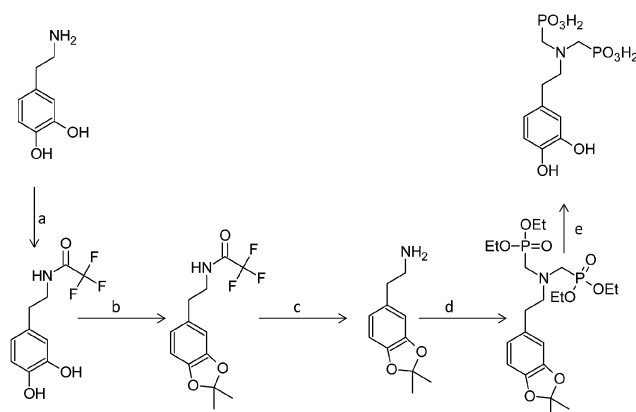
Crystalline ZnAl-chloride LDH (ZnAl-Cl) was synthesized by modifying the "Urea-method".¹⁷ ZnCl_2 (13.637 g, 100 mmol), $\text{AlCl}_3 \cdot 6\text{H}_2\text{O}$ (10.505 g, 43.5 mmol) and urea (10.44 g, 173.82 mmol) were refluxed in 300 mL of deionized water for 24 h. The precipitate was centrifuged and washed three times with deionized water. The Zn–Al molar ratio was evaluated by means of ICP analysis and the water content was evaluated by thermogravimetric analysis yielding the following formula $[\text{Zn}_{0.67}\text{Al}_{0.33}(\text{OH})_2]\text{Cl}_{0.33} \cdot 0.6\text{H}_2\text{O}$.

Synthesis of ZnAl/ $\text{H}_2\text{P}_2\text{O}_6\text{DOPA}$

In a microwave tube ZnAl-Cl (750 mg) was dispersed in 6.5 mL of H_2O . Dopamine (417 mg, 1.22 mmol) was dissolved into a solution of 1 mL of KOH 2 M and added to LDH-Cl. The mixture was then heated at 120 $^\circ\text{C}$ for 45 minutes under nitrogen using normal absorption into a Biotage initiator 2.5 microwave oven. The resulting solid was centrifuged, washed twice with deionized water and dried at 50 $^\circ\text{C}$ for 6 h.

Synthesis of Au@ZnAl/ $\text{H}_2\text{P}_2\text{O}_6\text{DOPA}$

8 mL of a solution of NaAuCl_4 in water (0.0125 M, 4.5 mg mL^{-1}) was added slowly to a suspension of 100 mg of LDH containing



Scheme 1 Synthetic procedure to prepare $\text{H}_4\text{P}_2\text{O}_6\text{DOPA}$. Reagents, conditions and yields: (a) CF_3COOMe , Et_3N in MeOH , 12 h r.t., 86%; (b) 2,2-dimethoxypropane, *p*-TsOH in benzene, 4 h reflux, 90%; (c) $\text{LiOH} \cdot \text{H}_2\text{O}$ in $\text{THF}/\text{H}_2\text{O}$ 4 h r.t., 87%; (d) HCOH , diethylphosphite, 2 h 120 $^\circ\text{C}$, 55%; (e) HCl 37% 12 h reflux, 100%.

dopamine in 10 mL of CO₂-free deionized water. The reaction mixture turned into dark red color and was stirred for 12 h at r.t. under nitrogen and protected from light. The resulting solid was centrifuged, washed twice with deionized water and dried at 50 °C for 6 h.

Results and discussion

The surface of ZnAl-Cl was functionalized by using microwaves with anions of H₄P₂O₆DOPA obtained by partial deprotonation of the phosphonic group in 2 M KOH. A 2 : 1 molar ratio of KOH/H₄P₂O₆DOPA (4 acid protons per mol of phosphonic acid) was used with the aim of obtain H₂P₂O₆DOPA²⁻ di-anion in which two acid protons are maintained.

The H₂P₂O₆DOPA²⁻ anions exchange the Cl⁻ anions of the LDH and, upon dehydration at 50 °C, a grafting reaction between the acid P-OH and the OH- groups of the lamella occurs. The appearance of a small absorption band around 1000 cm⁻¹ can be ascribed to fully deprotonation of P-OH groups and the formation of M-O-P bonds (see Fig. 1S, ESI†).¹⁸ The loss of one water molecule per phosphonic group also occurred. The diffraction pattern of ZnAl/H₂P₂O₆DOPA (Fig. 2) is typical of the ZnAl-Cl, having an interlayer distance of 7.75 Å, indicating that the exchange reaction of H₂P₂O₆DOPA involved only the LDH surface and that did not occur into the interlayer region of the LDH.

Fig. 1 schematizes the exchange/grafting reaction of the H₂P₂O₆DOPA anions onto the surface of hexagonal ZnAl-Cl microcrystals. The content of Zn, Al, P, N, O, C and H in ZnAl/H₂P₂O₆DOPA was determined by ICP, CHN elemental analysis and TXRF, considering a quantitative grafting reaction the composition resulted [Zn_{0.67}Al_{0.33}(OH)_{1.896}Cl_{0.226}(P₂O₆DOPA)_{0.052}·0.23H₂O. Analysis calculated C : H : N for ZnAl/H₂P₂O₆DOPA was 6.01 : 2.92 : 0.70 and found 5.96 : 3.11 : 0.71.

A NaAuCl₄ aqueous solution was added to a ZnAl/H₂P₂O₆DOPA aqueous dispersion, the mixture turned into dark red color indicating that the Au(III) ions were quickly reduced to gold nanoparticles on the LDH surface by the catechol groups. X-ray diffraction pattern of the recovered composite Au@LDH/H₂P₂O₆DOPA shows (Fig. 2) the reflections of cubic gold beside the ZnAl-Cl reflections.

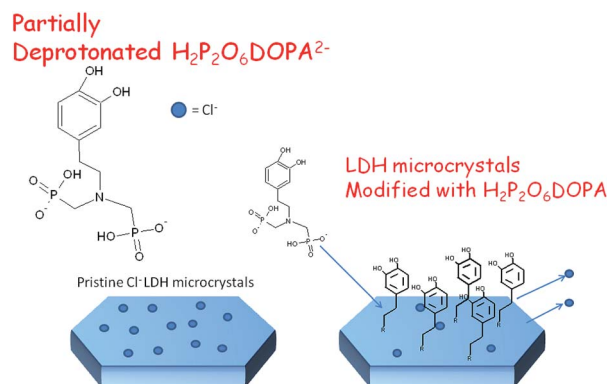


Fig. 1 Schematic representation of the exchange/grafting reaction of H₂P₂O₆DOPA anions onto the LDH surface.

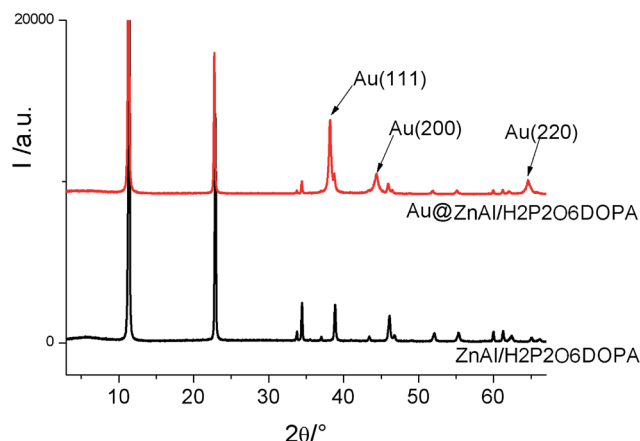


Fig. 2 XRPD patterns of the ZnAl/H₂P₂O₆DOPA and of Au@ZnAl/H₂P₂O₆DOPA LDH.

Rietveld refinement of the Au@ZnAl/H₂P₂O₆DOPA diffraction pattern allowed to get information on the volume weighted crystalline domain size of Au nanoparticles and on the relative quantitative phase analysis of the two components.

Microstructural analysis was performed by using the GSAS program.¹⁹ Table 1S† reports the instrumental and refinement details. First, the instrumental contribution to the peak broadening was previously evaluated by the Rietveld refinement of the profile of lanthanum hexaboride (LaB₆), as an external peak profile standard. We assumed that the standard was not affected by microstrain, and the instrumental broadening was modeled by the refinement of W and Y peak shape parameters for Gaussian and Lorentzian contributions, respectively. Coherent domain size (volume weighted) parallel (D_{\parallel}) and perpendicular (D_{\perp}) to the (200) and to the (111) directions was calculated by using the following expressions

$$D_{\parallel} = 1800\lambda/\pi(X + X_e) \text{ and } D_{\perp} = 1800\lambda/\pi X$$

Microstrain as source of peak broadening was also considered. In order to give an average strain value along the selected direction a simple strain model (%) was also used by refining the Gaussian and the Lorentzian contribution Y , Y_e and Y_i where Y_i is the experimental instrumental contribution obtained with the LaB₆ standard. The equation for the strain% ϵ_{\parallel} and ϵ_{\perp} to the selected broadening axes are

$$\epsilon_{\parallel} = (\pi/18\,000)(Y + Y_e - Y_i) \text{ and } \epsilon_{\perp} = (\pi/18\,000)(Y - Y_i)$$

where λ is the wavelength and X and X_e are two terms related to the Lorentzian contribution of the size broadening effect.

The calculation gave as results an average $D_{\parallel 200}$ crystalline domain size of about 16 nm whereas the $D_{\perp 200}$ is about 100 nm.

The $D_{\parallel 111}$ and $D_{\perp 111}$ were 34 and 12 nm respectively. These data roughly indicate the crystalline domain sizes measured along and perpendicular to the selected directions and generally they do not correspond to the observed size from electron microscope images. In our case a size anisotropy perpendicular

to the (200) seems to be present. Concerning the microstrain the only predominant effect, nicely related to the peak broadening effect, can be detected only on the direction perpendicular to (200) which is $\varepsilon_{\perp} (\times 10^3) = 1.9$. The calculation carried out on different directions did not give any valuable result. This means that, along that direction, strain efficiently contributes to the broadening. The high D value found for that plane (200) is then affected by the strain contribution and it is probably overestimated. Quantitative phase analysis was carried out by using the Bish and Howard formula.²⁰

$$Wm = \frac{a_m S_m}{\sum_{k=1}^{k=m} a_k S_k}$$

where Wm and a_k are the weighed fraction of the m^{th} component in the sample and its calculated density, respectively; a_k is given as follows: $a_k = Z_k M_k U_k$ where Z_k , M_k , and U_k are the number of chemical formula units in a unit cell, the molecular weight, and the unit-cell volume, respectively. The calculation, in absence of amorphous phases, gave as result 22% of Au.

Assuming that the only amorphous contribution to the mixture can be ascribed to the presence of the $\text{H}_2\text{P}_2\text{O}_6\text{DOPA}$ anions coating (calculated on the basis of the molar fraction = 18.5 wt%), the normalized relative phase weight percentages were LDH = 64.9%, Au = 16.6%.

The value calculated from quantitative analysis is 0.138 mol of Au/mol of Au@LDH/ $\text{H}_2\text{P}_2\text{O}_6\text{DOPA}$ that is in good agreement with the value found by elemental analysis (ICP and TXRF) (0.127 mol of Au/mol of compound). The elemental analysis of Au@ZnAl/ $\text{H}_2\text{P}_2\text{O}_6\text{DOPA}$ showed that the content of Zn and Al was different from the ZnAl/ $\text{H}_2\text{P}_2\text{O}_6\text{DOPA}$ starting material. In particular after Au deposition the solid was enriched in Al. The oxidation of catechol groups to quinone groups occurs with the formation of H^+ ions that locally decrease the pH.²¹ LDHs at low pH value can undergo to a partial dissolution with a preferential leaching of the more soluble cation that is Zn. This process on the one hand leads to a partial dissolution of LDH on the other hand drives the catechol oxidation reaction to right promotion the formation of metallic gold clusters. Considering that the maximum aluminium molar fraction possible for LDH is 0.40 a segregation of $\text{Al}(\text{OH})_3$ was hypothesized and the composition of the solid was then written as $[\text{Zn}_{0.60}\text{Al}_{0.40}(\text{OH})_{1.834}]\text{Cl}_{0.234}(\text{P}_2\text{O}_6\text{DOPA})_{0.083}\text{Au}_{0.127} \cdot 0.3\text{H}_2\text{O} + 0.04 \text{Al}(\text{OH})_3$. Analysis calculated for Au@ZnAl/ $\text{H}_2\text{P}_2\text{O}_6\text{DOPA}$ C : H : N was 6.59 : 2.41 : 0.77 and found 6.38 : 2.77 : 0.77.

Rietveld plot is shown in Fig. 3 whereas the complete refinement parameters and procedures are reported in ESI, Table 1S.†

FE-SEM and TEM images of the pristine LDH and of the Au@LDH/ $\text{H}_2\text{P}_2\text{O}_6\text{DOPA}$ microcrystals are shown in Fig. 4.

Fig. 4a (FE-SEM) shows the pristine ZnAl-LDH microcrystals; it should be remarked that the surface of the crystals was well polished. After the modification with $\text{H}_2\text{P}_2\text{O}_6\text{DOPA}$ anions the crystal surface turned into dark colour and, at higher magnification degree (Fig. 4c and d) it also became corrugated. Indeed, small globular structures of size < than 10 nm were

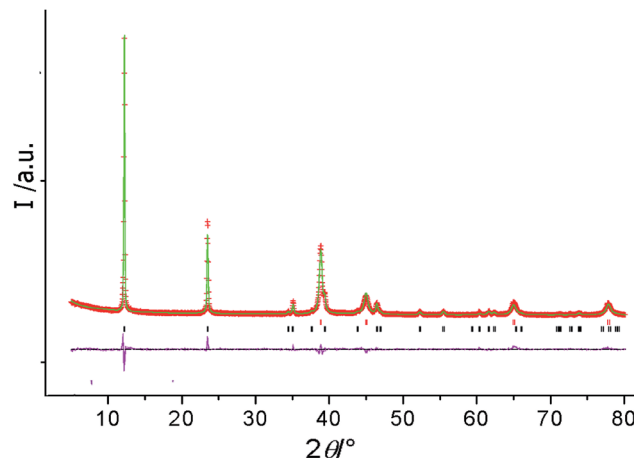


Fig. 3 Rietveld plot of Au@ZnAl/ $\text{H}_2\text{P}_2\text{O}_6\text{DOPA}$ LDH.

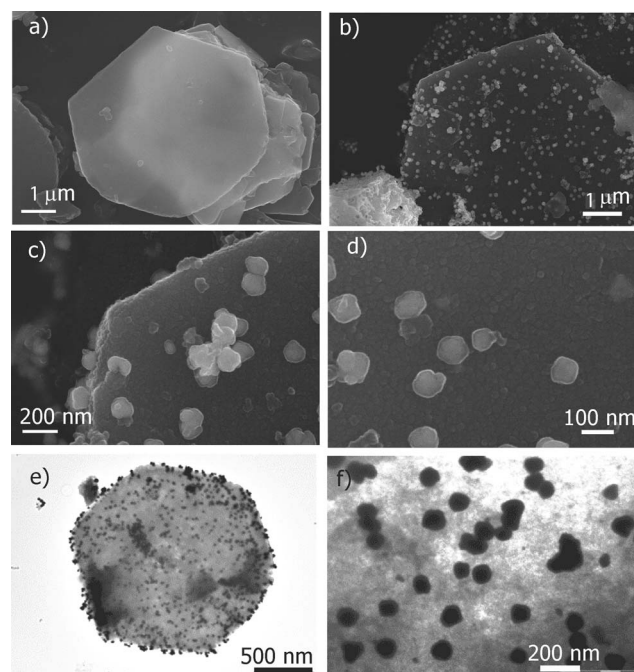


Fig. 4 FE-SEM (a–d) and TEM (e–f) images of pristine (a), and modified (b–f) ZnAl-LDH microcrystals.

homogeneously present over the entire surface. These structures cannot be attributed to smaller gold clusters as they are not present in the equivalent TEM images which are more sensitive to the atomic weight (Fig. 4e and f).

This also suggests that the modification of the LDH microcrystals with $\text{H}_2\text{P}_2\text{O}_6\text{DOPA}$ anions occurred efficiently with a homogeneous covering of the surface with the organic molecules.

Gold NPs are well dispersed over the entire LDH crystal surface and apparently they seem to have a spherical shape with a narrow size distribution ranging from 60 to 90 nm. Some of them are aggregated in larger clusters formed by 4 or 5 NPs each.

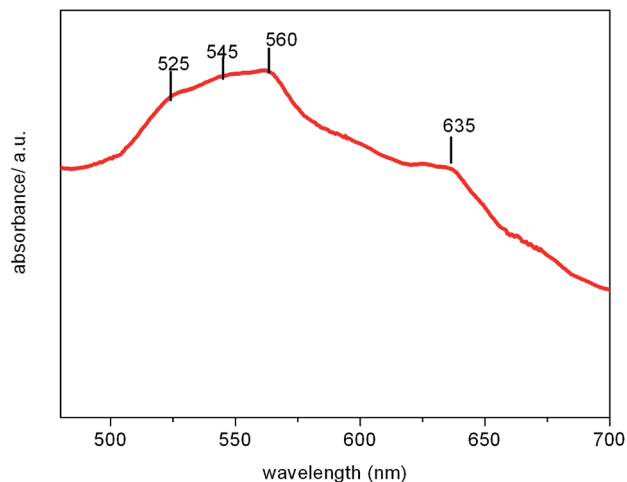


Fig. 5 Uv-vis spectrum of Au@ZnAl/H₂P₂O₆DOPA. The SPR signals at 525, 545 and 560 nm are indicated.

Surface Plasmonic Resonance (SPR) spectra were also collected on the bulk solid. The absorption spectrum is reported in Fig. 5.

SPR spectrum shows three distinct peaks (determined by second derivative of the curve) at 525, 545 and 560 nm. This confirms the polydisperse nature of the gold nanoclusters.

According to El-sayed and Link²² the position of the SPR signals can be related with the average particle size for mono-disperse systems. In our case the predominant 560 nm signal is indicative of 70 to 90 nm size gold clusters. The signals at 545 and 525 nm can be related to 50 and 25 nm clusters size respectively. A fourth signal around 635 nm can be ascribed to one of the absorption modes of quinone or metal coordinated hydro-quinones.²³

These data are in good agreement with the FE-SEM and TEM images. LDH as solid supports for AuNPs have been recently reported from other authors and these materials were mainly employed for catalytic purposes.²⁴

The NPs were grown on the LDH crystal surface by using conventional reduction methods involving citrate or urea as precipitating agent. The average size of AuNPs reported in other papers was generally lower than that reported in our work (5 to 20 nm, vs. 40 to 90 nm). Nevertheless, respect to the conventional methods, the catechol coating LDHs appear to be more efficient in terms of Au(0) conversion, allowing the precipitation of higher amount of Au, expressed as weight%.

Moreover, found density of Au NPs onto the LDH crystal surface by us was generally higher than that reported in other papers. The effort to improve the size/shape tuning of the gold cluster, by changing the initial amount of Au and other parameters like solvents and temperature, will be carried out in the near future.

Conclusions

In this paper the organic synthesis of a catechol-bearing phosphonic acid, derived from dopamine, has been reported with

respect to dopamine, the reactivity of this novel phosphonate is drastically changed due to the non availability of the -NH₂ which precludes the possibility of self-polymerization into polydopamine.

The H₂P₂O₆DOPA anions have been then used to uniformly coat the surface of well crystallized LDH hexagonal crystals, the exposed catechol groups operating as the redox agent for the stabilization of polydisperse gold NPs. Respect to the conventional methods, this strategy is “template free” and allows to increase the absolute amount of gold nanoclusters onto the LDH surface. However, the disadvantage of this system resides in the scarce control of the gold NPs size and shape. We plan to address further applications of the catechol-bearing LDH in different fields, like the grafting of magnetic NPs and the complexation of catalytic metals and/or luminescent lanthanide ions for advanced applications in heterogenous catalysis, theranostic and imaging.

Acknowledgements

F.C. and M. N. thank Project FIRB 2010 no. RBFR10CWDA_003 for the financial support.

Notes and references

- (a) S. Callier, M. Snapyan, S. L. Crom, D. Prou, J.-D. Vincent and P. Vernier, *Biol. Cell*, 2003, **95**, 489–502; (b) A. Zhang, J. L. Neumeyer and R. J. Baldessarini, *Chem. Rev.*, 2007, **107**, 274–302.
- M. Brenner and V. Hearing, *J. Photochem. Photobiol.*, 2008, **84**, 539–549.
- (a) K. G. Alley, G. Poneti, P. S. D. Robinson, A. Nafady, B. Moubarak, J. B. Aitken, S. C. Drew, C. Ritchie, B. F. Abrahams, R. K. Hocking, K. S. Murray, A. M. Bond, H. H. Harris, L. Sorace and C. Boskovic, *J. Am. Chem. Soc.*, 2013, **135**, 8304–8323; (b) A. Dei, G. Poneti and L. Sorace, *Inorg. Chem.*, 2010, **49**, 3271–3277.
- (a) J. H. Waite, *Int. J. Adhes. Adhes.*, 1987, **7**, 9–14; (b) J. H. Waite, *Integr. Comp. Biol.*, 2002, **42**, 1172–1180.
- (a) H. Hartati, M. Santoso, S. Triwahyono and D. Prasetyoko, *Bull. Chem. React. Eng. Catal.*, 2013, **8**, 14–33; (b) I. Reyero, G. Arzamendi and L. M. Gandía, *Key Eng. Mater.*, 2013, **571**, 1–26.
- (a) Y. Long, J. Wu, H. Wang, X. Zhang, N. Zhao and J. Xu, *J. Mater. Chem.*, 2011, **21**, 4875–4881; (b) G. J. Gou, L. E. Dong, F. J. Bao, Z. Y. Wang, L. Jiao, J. Huang, Y. Sun and B. Bing Xue, *Appl. Mech. Mater.*, 2013, **320**, 495–504.
- D. E. Fullenkamp, J. G. Rivera, Y. Gong, K. H. A. Lau, L. He, R. Varshney and P. B. Messersmith, *Biomaterials*, 2012, **33**, 3783–3791.
- Y. Lee, H. Lee, Y. Beom Kim, J. Kim, T. Hyeon, H. Wook Park, P. B. Messersmith and T. G. Park, *Adv. Mater.*, 2008, **20**, 4154–4157.
- (a) A. Vaccari, *Appl. Clay Sci.*, 1999, **14**, 161–168; (b) M. Turco, G. Bagnasco, U. Costantino, F. Marmottini, T. Montanari, G. Ramis and G. Busca, *J. Catal.*, 2004, **228**, 43–55; (c) T. Montanari, M. Sisani, M. Nocchetti, R. Vivani,

- M. Concepcion Herrera Delgado, G. Ramis, G. Busca and U. Costantino, *Catal. Today*, 2010, **152**, 104–109; (d) G. Busca, U. Costantino, T. Montanari, G. Ramis, C. Resini and M. Sisani, *Int. J. Hydrogen Energy*, 2010, **35**, 5356–5366; (e) A. Fronzo, C. Pirola, A. Comazzi, C. L. Bianchi, A. Di Michele, R. Vivani, M. Nocchetti, M. Bastianini, D. C. Boffito and F. Galli, *Fuel*, 2014, **119**, 62–69; (f) I. Reyero, G. Arzamendi and L. M. Gandía, *Key Eng. Mater.*, 2013, **571**, 1–26.
- 10 (a) *Clays and Health Clays in Pharmacy, Cosmetics, Pelotherapy, and Environmental Protection*, Special Issue of Appl. Clay Sci., ed. M. I. Carretero and G. Lagaly, 2007, vol. 36; (b) V. Ambroggi, V. Ciarnelli, M. Nocchetti, L. Perioli and C. Rossi, *Eur. J. Pharm. Sci.*, 2009, **73**, 285–291; (c) LDH in physical, chemical, bio-chemical and life sciences in Developments in Clay Science – Volume 5B *Handbook of Clay Science: Techniques and Applications*, ed. F. Bergaya and G. Lagaly, 2013, vol. 5B; (d) L. Li, W. Gu, J. Chen, W. Chen and Z. P. Xu, *Biomaterials*, 2014, **35**, 3331–3339; (e) V. Rives, M. del Arco and C. Martín, *Appl. Clay Sci.*, 2014, **88–89**, 239–269.
- 11 (a) H. H. Q. Wang, Z. Tay, J. Zhong, J. Luo and A. Borgna, *Energy Environ. Sci.*, 2012, **5**, 7526–7530; (b) O. Aschenbrenner, P. McGuireb, S. Alsamaq, J. Wang, S. Supasitmongkola, B. Al-Durib, P. Styringa and J. Wood, *Chem. Eng. Res. Des.*, 2011, **89**, 1711–1721.
- 12 F. L. Theiss, S. J. Couperthwaite, G. A. Ayoko and R. L. Frost, *J. Colloid Interface Sci.*, 2014, **417**, 356.
- 13 (a) U. Costantino, V. Ambroggi, L. Perioli and M. Nocchetti, *Microporous Mesoporous Mater.*, 2008, **107**, 149–160; (b) J.-M. Oh, S.-J. Choi, G.-E. Lee, S.-H. Han and J.-H. Choy, *Adv. Funct. Mater.*, 2009, **19**, 1617–1624; (c) E. Ruiz-Hitzky, P. Aranda, M. Darder and G. Rytwo, *J. Mater. Chem.*, 2010, **20**, 9306–9321; (d) L. Perioli, V. Ambroggi, M. Nocchetti, M. Sisani and C. Pagano, *Appl. Clay Sci.*, 2011, **53**, 696–703; (e) U. Costantino, F. Costantino, F. Elisei, L. Latterini and M. Nocchetti, *Phys. Chem. Chem. Phys.*, 2013, **15**, 13254–13269; (f) M. Nocchetti, A. Donnadio, V. Ambroggi, P. Andreani, M. Bastianini, D. Pietrella and L. Latterini, *J. Mater. Chem. B*, 2013, **1**, 2383–2393.
- 14 K. Moedritzer and R. R. Irani, *J. Org. Chem.*, 1966, **31**, 1603–1606.
- 15 Z. Liu, B. Hu and P. B. Messersmith, *Tetrahedron Lett.*, 2010, **51**, 2403.
- 16 A. A. Prishchenko, M. V. Livantsov, O. P. Novikova, L. I. Livantsova and V. S. Petrosyan, *Heteroat. Chem.*, 2010, **21**, 430–440.
- 17 (a) U. Costantino, F. Marmottini, M. Nocchetti and R. Vivani, *Eur. J. Inorg. Chem.*, 1998, **10**, 1439–1446; (b) M. Bastianini, D. Costenaro, C. Bisio, L. Marchese, U. Costantino, R. Vivani and M. Nocchetti, *Inorg. Chem.*, 2012, **51**, 2560.
- 18 (a) U. Costantino, M. Casciola, L. Massinelli, M. Nocchetti and R. Vivani, *Solid State Ionics*, 1997, **97**, 203–212; (b) U. Costantino, S. Clementi, M. Nocchetti and R. Vivani, *Mol. Cryst. Liq. Cryst. Sci. Technol., Sect. A*, 1998, **311**, 207–210.
- 19 C. Larson and R. B. von Dreele, *Generalized Crystal Structure Analysis System*, Los Alamos National Laboratory, Los Alamos, NM, 2001.
- 20 D. L. Bish and S. A. Howard, *J. Appl. Crystallogr.*, 1998, **21**, 86–91.
- 21 S. A. Mechler, A. A. J. Torriero, A. Nafady, C. Y. Lee, A. M. Bond, A. P. O'Mullane and S. K. Bhargava, *Colloids Surf., A*, 2010, **370**, 35–41.
- 22 S. Link and M. A. El-Sayed, *J. Phys. Chem. B*, 1999, **103**, 4212–4217.
- 23 M. J. Sever and J. J. Wilker, *Dalton Trans.*, 2004, 1061–1072.
- 24 (a) J. Zhao, X. Kong, W. Shi, M. Shao, J. Han, M. Wei, D. G. Evans and X. Duan, *J. Mater. Chem.*, 2011, **21**, 13926–13933; (b) F. Zhang, X. Zhao, C. Feng, B. Li, T. Chen, W. Lu, X. Lei and S. Xu, *ACS Catal.*, 2011, **1**, 232–237; (c) Y. Wang, D. Zhang, M. Tang, S. Xu and M. Li, *Electrochim. Acta*, 2010, **55**, 4045–4049.